Parallelization of microfluidic flow-focusing devices

Esther Amstad, Xiaoming Chen, Max Eggersdorfer, Noa Cohen, Thomas E. Kodger, Carolyn L. Ren, and David A. Weitz

Phys. Rev. E **95**, 043105 — Published 14 April 2017

DOI: 10.1103/PhysRevE.95.043105

Parallelization of microfluidic flow-focusing devices

Esther Amstad,[1,2*] Xiaoming Chen,[3] Max Eggersdorfer,[1] Noa Cohen,[1] Thomas E. Kodger,[4] Carolyn L Ren, [3] David A. Weitz[1,4]

[1] *School of Engineering and Applied Sciences, Harvard University, USA*
[2] *Institute of Materials, Ecole Polytechnique Fédérale de Lausanne (EPFL), Switzerland*
[3] *Department of Mechanical & Mechatronics Engineering, University of Waterloo, Canada*
[4] *Department of Physics, Harvard University, USA*

Received (in XXX, XXX) Xth XXXXXXXXX 200X, Accepted Xth XXXXXXXXX 201X)

Microfluidic flow-focusing devices offer excellent control over fluid flow, enabling formation of drops with a narrow size distribution. However, the throughput of microfluidic flow-focusing devices is limited and scale-up through operation of multiple drop makers in parallel often compromises the robustness of their operation. We demonstrate that parallelization is facilitated if the outer phase is injected from the direction opposite to that of the inner phase, because the fluid injection flow rate, where the drop formation transitions from the squeezing into the dripping regime, is shifted towards higher values.

DOI: XXXXXXXXXX PACS number(s): 47.61.-k, 47.61.Jd, 47.55.db

I. INTRODUCTION

Drops are often used as vessels to conduct screening assays,[1] synthesize microparticles,[2] and perform single cell analysis.[3] Many of these applications require drops with a narrow size distribution. Microfluidic devices offer a good control over the drop size and allow production of monodisperse drops. For example, microfluidic flow-focusing devices enable the production of drops with a coefficient of variation, defined as the standard deviation of their size distribution divided by the mean drop size, of 1%-2%.[4] Junctions of such flow-focusing devices typically consist of a pair of inlets intersecting the main channel at an angle of 90° or less.[5-7] These devices operate at flow rates with a very low Capillary number, $Ca = \frac{\mu_o q_o}{\gamma A_o}$, which describes the competition between viscous forces and interfacial tension forces; here $\mu_o$is the viscosity of the outer phase, $q_o$its flow rate, A_o its cross-sectional area, and γ the interfacial tension. In this case, drops form in the squeezing regime where the inner phase penetrates into the junction and blocks it almost entirely, thereby preventing the outer phase from entering the main channel before the inner phase starts to neck. In this regime, the dynamics of drop breakup is entirely controlled by the flow rate of the outer phase,[8] such that the drop size depends on the flow rate of the outer phase,[6, 9] its viscosity and surface tension,[10] and the channel geometry.[7, 11, 12] However, the necking process, which eventually leads to drop formation, is slow, limiting the maximum drop generation frequency and hence the throughput. The drop generation frequency can be increased if an additional thin orifice is added after the cross-junction.[13] However, a small orifice increases the risk of blocking the microchannel, thereby compromising the operation robustness of this device. The throughput can be improved by increasing the flow rate of the inner phase, such that Ca increases. If Ca exceeds some value, the drop generation transitions into the dripping regime, where the inner phase only partially blocks the junction. The break-up of drops is then caused by the classic Rayleigh-Plateau instability[14] and their size is influenced by flow rates of the inner and outer phases, Ca, and the channel geometries. Because the size of drops formed in the dripping regime depends on many more parameters than those produced in the squeezing regime, their size distribution is usually broader. As a result, production of monodisperse drops is more robust if devices are operated in the squeezing regime where the throughput is very low. To increase throughput, multiple drop makers can be operated simultaneously through parallelization.[15-20] However, this compromises the robustness of their operation because the failure of any one single drop maker causes failure of the entire device. Moreover, because the drop size depends on fluid flow rates[6] and small variances across a parallelized device inevitably occur, parallelization often broadens the drop size distribution. To overcome this shortcoming, new device geometries that facilitate parallelization of individual flow-focussing devices are needed.

In this paper, we introduce a new flow-focusing junction geometry where the outer phase is injected from the opposite direction to that of the inner phase. We investigate the influence of the junction geometry on the size of drops formed in these devices. Moreover, we demonstrate that the new junction geometry shifts the fluid flow rates where drop formation transitions from the squeezing into the dripping regime towards higher values. The resulting enlarged flow rate regime where drops form in the squeezing regime greatly facilitates their parallelization.

II. RESULTS

We produce microfluidic flow-focusing devices from poly(dimethyl siloxane) (PDMS) using soft lithography;[21] they contain one inlet for the inner phase and one inlet for the outer phase. The inlet for the outer phase supplies two channels that intersect the main channel at an angle θ. We fabricate three types of devices with θ = 135°, 45°, and 90°, as shown by the optical micrographs in Figures 1a, 1b, and 1c. All channels have a square cross-section that is 40 μm wide and 40 μm tall and we keep the volume of the intersection constant at 64,000 μm^3.

To produce drops, channel walls must be non-wetting for the inner phase. Here, we produce aqueous drops in perfluorinated oil and we treat the channel walls with a perfluorinated oil (HFE7500) containing 1 vol% of a perfluorinated trichlorosilane. If we produce aqueous drops in a hydrocarbon-based oil, we treat the channel walls with a trichlorododecylsilane and if we produce oil drops in water, we treat the channel walls with polyelectrolytes. We use HFE7500 as an outer phase and add 1 vol% of a perfluorinated surfactant to stabilize the emulsion drops;[22] this phase has a viscosity of 1 mPa s. We use an aqueous solution containing 2 vol% poly(ethylene glycol) (PEG, M_w = 6 kDa) as an inner phase; this phase has a viscosity of 2 mPa s. The interfacial tension between the two fluids is 5 mN/m. We inject both fluids into the device using syringe pumps, which may result in small variations in fluid flow rates,[23, 24] which could influence the polydispersity of drops. To minimize the effect of flow rate variations caused by syringe pumps, we determine the diameter of 500 – 1000 drops, which are formed within approximately 1 s and report their mean value and standard deviation.[23]

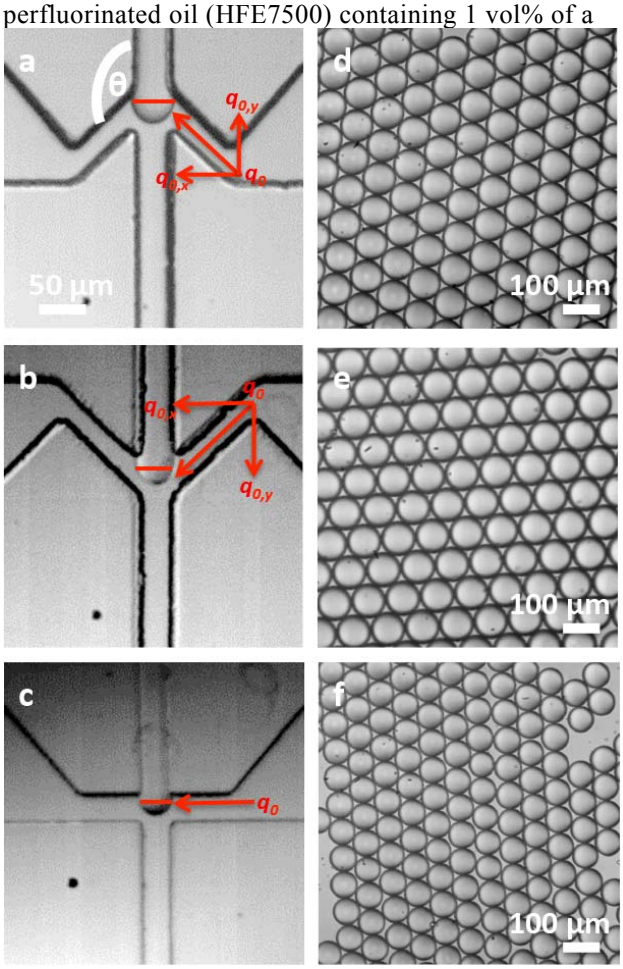

Figure 1: (a-c) Optical micrographs of microfluidic flow-focusing devices. The angle between the inlet of the outer phase and the main channel, θ, is (a) 135°, (b) 45° and (c) 90°. (d-f) Optical micrographs of drops produced in devices with θ = (d) 135°, (e) 45° and (f) 90°, respectively. The viscosity of the inner phase is 8 mPas, that of the outer phase is 1 mPas. The flow rate of the inner phase is 100 μL/h, that the outer phase is 1 mL/h. Drops have diameters of (a) 75 ± 2 μm, (b) 67 ± 2 μm, and (c) 41 ± 3 μm.

To investigate the mechanism by which emulsion drops form in different flow-focusing junction geometries, we visualize this process using a high-speed camera operated at 10,000 frames per second. If we inject the outer phase from the opposite direction to the flow of the inner phase, such that θ = 135°, the leading end of the inner phase attains a semi-spherical shape when it enters the junction, as shown in the optical micrograph in Figure 1a. This leading end serves as a drop precursor that grows until its volume occupies the entire junction such that it impedes the flow of the outer phase. Thereby the precursor initiates the necking of the inner phase, which leads to drop pinch-off, as shown in movie S1. This behaviour is reminiscent for drops formed in the squeezing regime. These drops display a narrow size distribution, as shown in the optical micrograph in Figure 1d. Similarly, drop precursors formed in junctions with θ = 45° grow until their volume blocks the junction, when the outer phase initiates drop pinch-off, as shown in the optical micrograph in Figure 1b and movie S2. The resulting drops are of similar size and also display a very narrow size distribution, as shown in the optical micrograph in Figure 1e. The mechanism by which drops form in devices with θ = 90° is very similar, as shown in Figure 1c and movie S3. However, the size of these drops is significantly smaller, as shown in the optical micrograph in Figure 1f.

To investigate the reason for the different sizes of drops produced in different junctions, we quantify their average size and size distribution as a function of the fluid injection flow rates by analyzing the images using a Matlab code. We keep the flow rate of the outer phase, q_o, constant at 1000 μL/h such that Ca of the outer phase, Ca_o is 0.034. We vary the flow rate of the inner phase, q_i, between 100 μL/h and 1000 μL/h, such that the Ca of the inner phase, Ca_i, is between 0.0069

and 0.069. In all cases, we observe that drops form in the squeezing regime, in good agreement with drop formation reported for flow-focussing devices with θ = 90°.[25] The size of drops formed in junctions with θ = 45° is independent of the inner flow rate, as shown in Figure 2a. If formed in the squeezing regime, the drop volume is the sum of the volume of the drop precursor that penetrates into the junction before the necking starts and the volume that flows into the drop during its necking.[27-29] The inner flow rate only influences the necking time and this time is short, due to the high flow rate of the outer phase, as shown in movie S2. Therefore, the fluid volume that flows into the drop during its necking is very small compared to that of the precursor such that the drop volume is essentially that of the drop precursor; this volume is determined by the junction geometry and the outer flow rate and is independent of the inner flow rate.[28] Similarly, the size of drops produced in junctions with θ = 135° is independent of the inner flow rate if q_i > 300 µL/h. If q_i, is decreased from 300 µL/h ro 100 µL/h the drop size decreases by 6%, as shown in Figure 2a. In this case, q_i is so low that the inner phase flows back every time a drop pinches off, resulting in an unstable drop formation. This back-flow of the inner phase after drop pinch-off is much more pronounced if drops are formed in junctions with θ = 90°, as indicated by the steady increase in drop size with q_i until it reaches 700 µL/h. Hence, in these junctions, drop formation is only stable at q_i > 700 µL/h.

Drops produced in junctions with θ = 90° are significantly smaller than those made in the other junctions we tested, if formed at equal injection flow rates. We assign this difference to a change in the time required to initiate necking: If θ = 90°, the pressure build-up in the outer phase is much faster, such that the necking is initiated earlier, when the drop precursor volume is smaller. Therefore, we expect the drop volume to scale with the component of q_o, that is directed perpendicularly to the inner phase flow, $q_{o,x}$. To test this expectation, we vary q_o between 500 µL/h and 5000 µL/h, keeping q_i constant at 500 µL/h. As expected, the drop size decreases with increasing q_o for all geometries tested. In all cases, the size of drops produced in junctions with θ = 90° is smaller than that of drops produced in the other tested junctions. However, if we plot the drop sizes as a function of $q_{o,x}$, they are very similar independent of the junction geometry, as shown in Figure 2c. These results indicate that the time of the necking onset is influenced only by $q_{o,x}$.

The drop size depends on the time of the onset of the necking. We expect this time to depend on the viscosity of the outer phase. To test this expectation, we increase its viscosity ten-fold by adding 30 wt% of Krytox PGL107 such that the viscosity ratio, μ_i/μ_o is 0.2. Indeed, drops produced with this pair of fluids are smaller, indicating that the more viscous outer phase initiates the necking earlier, albeit the drop size difference is only 10%, as shown in Figure 2. This result is in good agreement with the viscosity-dependence of the size of drops produced in other microfluidic flow-focusing devices with θ = 90°.[10] For the same flow conditions, the size of drops generated in the devices with θ = 45° and θ = 135° are expected to be the same because the q_x of the outer phase flow rate are the same. Indeed, the sizes of drops produced in the devices with θ = 45° and θ = 135° are very similar if the viscosity of the outer phase is lower than the inner fluid, as shown by the solid symbols in Figure 2 (c). However, the size of drops generated in the devices with θ = 135° is larger than that of drops produced in devices with θ = 45° if the viscosity of the outer phase is increased 10-fold such that it is higher than that of the inner phase, as shown by the empty symbols in Figure 2. If the viscosity of the outer phase is higher than that of the inner phase, the meniscus of the inner fluid is pushed back every time a drop is pinched off in devices with θ = 135°. In devices with θ = 135°, the inner fluid is pushed back if the local underpressure at the meniscus of the inner fluid, caused by the drop pinch-off, is higher than the pressure at which fluid is injected in the liquid inlet.[30] The distance the meniscus is pushed back increases with increasing viscosity of the outer phase and with decreasing viscosity of the inner phase.[30] In devices with θ = 135°, the push-back is enhanced because the y-component of the outer fluid contributes to this push-back. Hence, if we increase the viscosity of the outer phase 10-fold, this push-back is much more pronounced in devices with θ = 135°. For the inner fluid to flow towards the junction, pressure must first be built-up. When the pressure is sufficiently high for the newly formed meniscus to flow into the junction with θ = 135°, the precursor penetrates into the junction where its cross-section perpendicular to the flow direction increases. Thereby, it forms a significantly larger precursor than in junctions with θ = 45°. The larger precursor requires more time to trigger the necking, thereby resulting in larger drop sizes, as shown by the open symbols in Figure 2 (c).

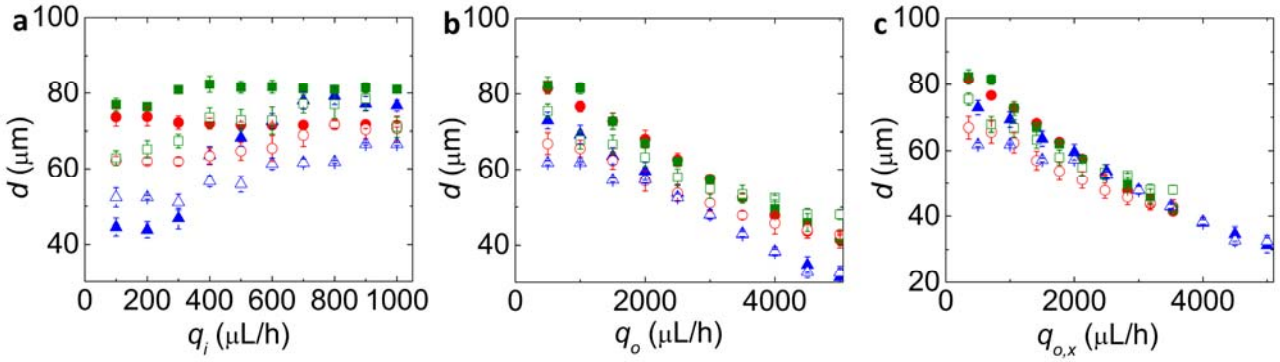

Figure 2: The size of drops produced in devices with θ = 45° (●), 90° (▲), and 135° (■), respectively. The viscosity of the inner phase is 2 mPas, that of the outer phase is 1 mPas (filled symbols) and 10 mPas (open symbols). (a) The flow rate of the outer phase is 1 mL/h. (b-c) Drop size as a function of the flow rate of the outer phase (b) and the velocity component of the outer phase perpendicular to the main channel (c). The flow rate of the inner phase is 500 μL/h.

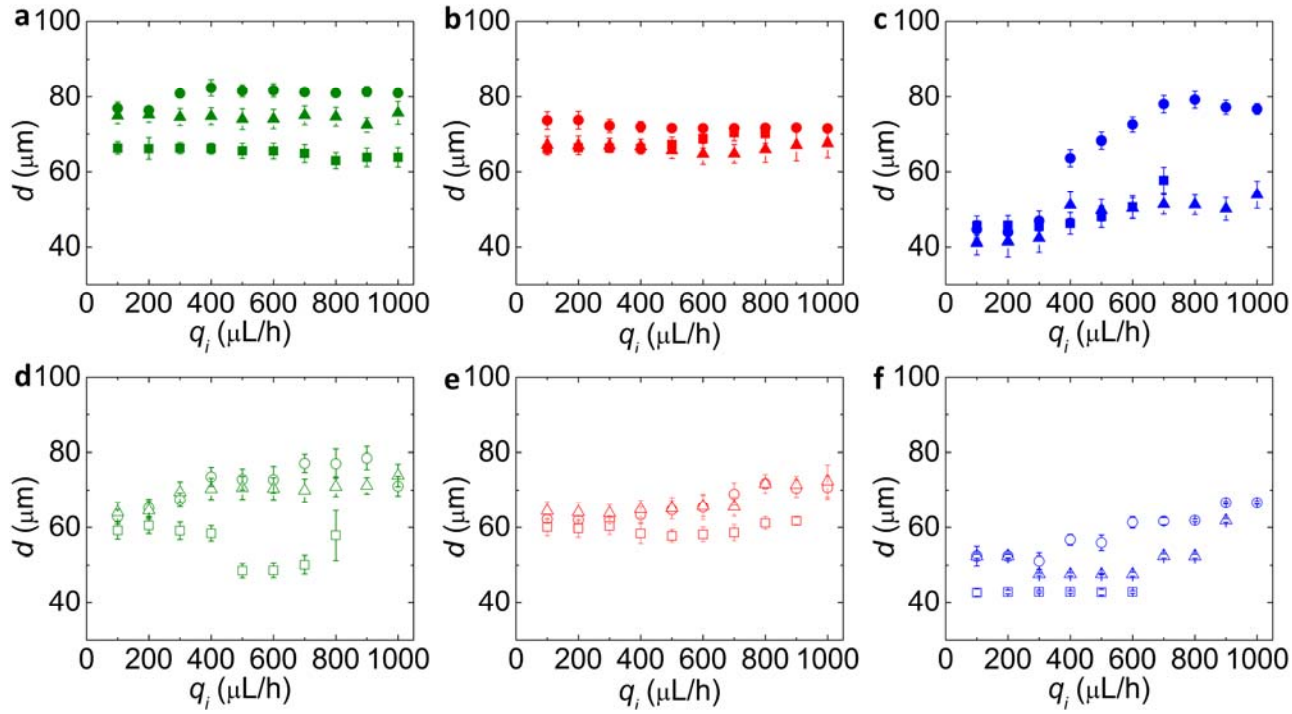

Figure 3: The size of drops produced in devices with θ = (a,d) 135°, (b,e) 45°, and (c,f) 90°C. The viscosity of the inner phase is 2 mPa s (circles), 8 mPa s (triangles), and 30 mPa s (squares). (a-c)The viscosity of the outer phase is 1 mPa s and (d-f) 10 mPa s. The flow rate of the outer phase is 1000 μL/h.

The timing of the necking onset is essentially determined by the outer phase. As a result, we expect it to be independent of the viscosity of the inner phase. Indeed, the size of drops formed in devices with θ = 135° remains nearly the same if we increase the viscosity of the inner phase four fold by increasing the PEG concentration to 20%, as shown by the triangles in Figure 3a. Even if we increase the viscosity of the inner phase to 30 mPa s by increasing the PEG concentration to 40 vol%, the drop size decreases by only 12%, as shown by the squares in Figure 3a. Differences in the sizes of drops generated in devices with θ = 45° are even smaller: The drop size varies by only 8% if we change the viscosity of the inner phase by a factor 15, as shown in Figure 3b. Similarly, the size of drops formed in junctions with θ = 90° is nearly independent of the viscosity of the inner phase for q_i > 400 μL/h, as shown in Figure 3c. By contrast, significant differences are observed for higher values of q_i. At these flow rates, the drop formation becomes much more stable at higher fluid flow rates if the viscosity of the inner phase is 8 mPa s or higher, such that their size does not increase abruptly at q_i = 400 μL/h. Hence, drops formed from solutions with higher viscosities are significantly smaller than those formed

from solutions with a viscosity of 2 mPa s, as shown in Figure 3c. Similar results are observed if the viscosity of the outer phase is increased to 10 mPa s. Drops composed of fluids with viscosities below 10 mPa s display nearly the same size, if produced in devices with θ = 135°, as shown by the empty symbols in Figure 3d. However, if the viscosity of the inner phase is increased to 30 mPas, inner phase starts to jet at flow rates as low as 400 µL/h, resulting in an abrupt change in drops size, as shown in Figure 3d. This transition into the jetting regime is not observed at such low flow rates in junctions with θ = 45° and θ = 90°, such that the viscosity of the inner phase has a much smaller effect on the drop size, as shown in Figures 3e and 3f.

To better understand the effect of the junction geometry on the drop size, we define an effective capillary number as ———————— where A is the cross-sectional area of the junction, the viscosity of the outer phase fluid, the flow rate of the outer phase fluid with its horizontal component as and vertical component as , and a fitting parameter that describes the influence of the viscous force caused by the y-component of the outer flow, $q_{o,y}$ on Ca_{eff}.

To determine the effective capillary number, we first consider the geometry with θ = 135°. Because the flow direction of is opposite to that of the inner phase fluid, the outer phase fluid exerts a force that counteracts the penetration of the inner phase into the main channel. Therefore, the force caused by the flow of prevents droplets from being sheared such that Ca_{eff} for the devices with θ = 135°, is — ——. The effective capillary number in devices with θ = 90° is higher, ——, and that in devices with θ = 45° is even higher, — ——. Because Ca_{eff} is smallest in devices with θ = 135°, we expect the transition from the squeezing into dripping regime in these devices to occur at higher injection flow rates.

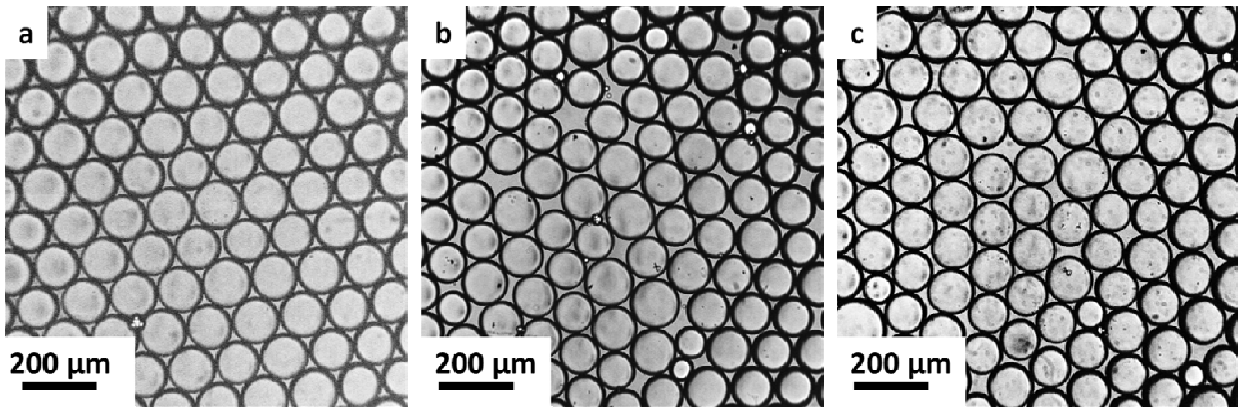

Figure 4: Optical micrographs of emulsion drops produced with 10 parallelized drop makers operated simultaneously. The angle θ between the outer and inner phase is (a) 135°, (b) 45° and (c) 90°. The drops have a diameter of (a) 86 ± 3 µm (CV = 7%), (b) 64 ± 6 µm (CV = 19%) and (c) 86 ± 5 µm (CV = 12%).

The influence of the shear force on the size of drops is much lower if they are produced in the squeezing regime than if made in the dripping regime. Therefore, we expect drops to display a significantly narrower size distribution if all drop makers operate in the squeezing. To operate all drop makers contained in parallelized devices in the squeezing regime the fluid flow rates in each drop maker must be below the rate, where drop formation transitions into the dripping regime. This is significantly facilitated, if the flow rate where this transition occurs is increased towards higher values. This is the case for drop makers with θ = 135°. Therefore, we expect these devices to produce drops with a narrower size distribution if parallelized. To test this expectation, we parallelize 10 drop makers, whose channels were 120 µm tall. We inject an aqueous solution cotaining 20 wt% PEG into a distribution channel that supplies each of the individual drop makers with the inner fluid. Similarly, we inject HFE7500 containing surfactants into a second distribution channels that supplies all drop makers with the outer fluid. Indeed, drops produced in devices with θ = 135° have a significantly narrower size distribution than those produced in the other junction geometries, as shown in the optical micrographs in Figure 4. These results suggest that all nozzles with θ = 135° operate in the squeezing regime. By contrast, we could not identify fluid flow rates where all 10 parallelized nozzles with θ = 45° or θ = 90° junctions operate in the squeezing regime. We assign this difference in the operation of individual drop makers to the gradient in fluid flow rates across the parallelized devices, that

exceeds the fluid flow rate range, where drops form in the squeezing regime. In this case, it is impossible to simultaneously operate all the drop makers in the squeezing regime. This would require optimization of the parallelization strategy, which is certainly possible to do but it is tedious. This example demonstrates the importance of junctions that enlarge the range of fluid flow rates where devices operate in the squeezing regime.

The new junction geometry offers an additional benefit: The two streams of the outer phase center the drop precursor while it is inside the junction, before it can touch any channel wall further downstream. Thereby, the outer phase minimizes the risk that the inner phase contacts one of the channel sidewalls, facilitating controlled drop formation from fluids that tend to wet channel walls. For example, the new junction geometry allows controlled formation of drops from silicon oils, which we failed to do in parallelized devices with $\theta = 45°$ or $\theta = 90°$; in all these cases, we coated the parallelized devices with Parylene to prevent their swelling.[26, 27] Hence, this small change in the junction geometry increases the robustness of the drop makers, further facilitating their parallelization.

III. CONCLUSIONS

Injection of the outer phase in the opposite direction to the flow of the inner phase enlarges the range of flow rates where microfluidic flow-focusing devices form drops in the squeezing regime. This small but effective change in the junction geometry makes the operation of flow focusing devices more robust which facilitates their parallelization. This small change in geometry adds an additional advantage: The two streams of the outer phase center the inner phase inside the junction, before drops form. Thereby, they minimize interactions of the inner phase with the channel walls and thus facilitate drop formation from fluids that tend to wet these walls.

ACKNOWLEDGEMENTS

This work was financially supported by Harvard MRSEC (DMR-0820484). The microfluidic devices were fabricated in the Center for Nanoscale Systems (CNS), a member of the National Nanotechnology Infrastructure Network (NNIN), which is supported by the National Science Foundation under NSF award no. ECS-0335765. CNS is part of Harvard University.

REFERENCES

See Supplemental Material at [*URL will be inserted by publisher*] for movies on the formation of drops in the three different junctions.

1 J. J. Agresti, et al., Proceedings of the National Academy of Sciences **107**, 4004 (2010).
2 T.-D. Dang, Y. H. Kim, H. G. Kim, and G. M. Kim, Journal of Industrial and Engineering Chemistry **18**, 1308 (2012).
3 A. Rotem, O. Ram, N. Shoresh, R. A. Sperling, A. Goren, D. A. Weitz, and B. E. Bernstein, Nature Biotechnology **33**, 1165 (2015).
4 P. Garstecki, I. Gitlin, W. DiLuzio, G. M. Whitesides, E. Kumacheva, and H. A. Stone, Appl. Phys. Lett. **85**, 2649 (2004).
5 S. L. Anna, N. Bontoux, and H. A. Stone, Applied Physics Letters **82**, 364 (2003).
6 T. Ward, M. Faivre, M. Abkarian, and H. A. Stone, Electrophoresis **26**, 3716 (2005).
7 A. R. Abate, A. Poitzsch, Y. Hwang, J. Lee, J. Czerwinska, and D. A. Weitz, Physical Review E **80** (2009).
8 P. Garstecki, H. A. Stone, and G. M. Whitesides, Physical Review Letters **94** (2005).
9 X. M. Chen, T. Glawdel, N. W. Cui, and C. L. Ren, Microfluidics and Nanofluidics **18**, 1341 (2015).
10 Z. Nie, M. Seo, S. Xu, P. C. Lewis, M. Mok, E. Kumacheva, G. M. Whitesides, P. Garstecki, and H. A. Stone, Microfluidics and Nanofluidics **5**, 585 (2008).
11 E. J. Vega, J. M. Montanero, M. A. Herrada, and A. M. Ganan-Calvo, Physics of Fluids **22** (2010).
12 B. Dollet, W. van Hoeve, J. P. Raven, P. Marmottant, and M. Versluis, Physical Review Letters **100** (2008).
13 L. Yobas, S. Martens, W. L. Ong, and N. Ranganathan, Lab on a Chip **6**, 1073 (2006).
14 K. J. Humphry, A. Ajdari, A. Fernandez-Nieves, H. A. Stone, and D. A. Weitz, Physical Review E **79** (2009).
15 M. B. Romanowsky, A. R. Abate, A. Rotem, C. Holtze, and D. A. Weitz, Lab on a Chip **12**, 802 (2012).
16 M. K. Mulligan and J. P. Rothstein, Microfluidics and Nanofluidics **13**, 65 (2012).
17 D. Conchouso, D. Castro, S. A. Khan, and I. G. Foulds, Lab on a Chip **14**, 3011 (2014).
18 T. Femmer, A. Jans, R. Eswein, N. Anwar, M. Moeller, M. Wessling, and A. J. C. Kuehne, ACS Appl. Mater. Interfaces **7**, 12635 (2015).
19 W. Li, J. Greener, D. Voicu, and E. Kumacheva, Lab on a Chip **9**, 2715 (2009).
20 T. Nisisako, T. Ando, and T. Hatsuzawa, Lab on a Chip **12**, 3426 (2012).
21 Y. N. Xia and G. M. Whitesides, Angewandte Chemie-International Edition **37**, 551 (1998).
22 C. Holtze, et al., Lab on a Chip **8**, 1632 (2008).
23 P. M. Korczyk, O. Cybulski, S. Makulska, and P. Garstecki, Lab on a Chip **11**, 173 (2011).
24 T. Glawdel and C. L. Ren, Microfluidics and Nanofluidics **13**, 469 (2012).

[25] T. Cubaud and T. G. Mason, Physics of Fluids **20** (2008).
[26] J. Flueckiger, V. Bazargan, B. Stoeber, and K. C. Cheung, Sensors and Actuators B-Chemical **160**, 864 (2012).
[27] H. C. Koydemir, H. Kulah, and C. Ozgen, Journal of Microelectromechanical Systems **23**, 298 (2014).
[28] V. Van Steijn, C.R. Kleijn and M.T. Kreutzer, *Lab Chip*, **10**, 2513-2518 (2010).
[29] X. Chen, T. Glawdel, N. Cui, and C. L. Ren, *Microfluid. Nanofluid*. **18**, 1341-1353 (2015).
[30] T. Glawdel, C. Elbuken, and C. L. Ren, Physical Review E, 85, 016322 (2012).